Journal of Process Control 22 (2012) 41–50

Contents lists available at SciVerse ScienceDirect

Journal of Process Control

journal homepage: www.elsevier.com/locate/jprocont

Model-based temperature control of a diesel oxidation catalyst

Olivier Lepreux [a,*], Yann Creff [a], Nicolas Petit [b]

[a] IFP Energies nouvelles, Technology, Computer Science and Applied Mathematics Division, BP 3, 69360 Solaize, France
[b] MINES ParisTech, Centre Automatique et Système, Mathématiques et Systémes, 60 bd. Saint-Michel, 75272 Paris Cedex 06, France

ARTICLE INFO

Article history:
Received 22 April 2011
Received in revised form 7 September 2011
Accepted 19 October 2011
Available online 23 November 2011

Keywords:
Reduced model
Distributed parameter systems
Delay systems
Diesel oxidation catalyst
Temperature control
Automotive exhaust aftertreatment systems

ABSTRACT

The problem studied in this article is the control of a DOC (diesel oxidation catalyst) as used in aftertreatment systems of diesel vehicles. This system is inherently a distributed parameter system due to its elongated geometry where a gas stream is in contact with a spatially distributed catalyst. A first contribution is a model for the DOC system. It is obtained by successive simplifications justified either experimentally (from observations, estimates of orders of magnitude) or by an analysis of governing equations (through asymptotic developments and changes of variables). This model can reproduce the complex temperature response of DOC output to changes in input variables. In particular, the effects of gas velocity variations, inlet temperature and inlet hydrocarbons are well represented. A second contribution is a combination of algorithms (feedback, feedforward, and synchronization) designed to control the thermal phenomena in the DOC. Both contributions have been tested and validated experimentally. In conclusion, the outcomes are evaluated: using the approach presented in this article, it is possible to control, in conditions representative of vehicle driving conditions, the outlet temperature of the DOC within $\pm 15\,^{\circ}$C.

1. Introduction

On most new diesel vehicles, increasing requirements regarding particulate matter emissions [1] are met using diesel particulate filters (DPF). This filter, located in the vehicle exhaust line, stores particulate matter until it is burnt in an active regeneration process [2]. During this phase, DPFs behave like potentially unstable reactors [3]. Consequently, their inlet temperature must be carefully controlled to prevent filter runaway. As is now exposed, this can be accomplished by the diesel oxidation catalyst (DOC).

In most current aftertreatment architectures [4], a DOC is placed upstream of the DPF in the vehicle exhaust line. To increase the DPF inlet temperature, reductants – mostly hydrocarbons (HC) – are oxidized in the DOC, which, in turn, increases the DOC outlet temperature, and therefore the DPF inlet temperature.

A DOC is a chemical system difficult to model and to control. Classical DOC models are usually composed of a dozen of coupled partial differential equations (PDEs) [5], which make difficult the development of model-based control laws. Experimentally, it has been observed that a step change on the inlet temperature propagates to the output of the system with large response times [6]. Depending on the engine outlet gas velocity, these response times significantly vary: they roughly decrease by a factor of 10 from idle speed to full load. Strategies that are commonly used to deal with this problem rely on controller gain look-up tables, which, in practice, are difficult and time-consuming to calibrate.

The purpose of this paper is to propose a simple model *dedicated to the DOC outlet temperature control during DPF regeneration* along with a control law. To achieve this, a simplification of the above-mentioned classical models is performed.

The paper is organized as follows. In Section 2.1 the control problem is exposed. In Section 2.2 the experimental setup is presented. The Section 3 presents a model describing the thermal responses properly. This model is physics-based. In Section 4, a control strategy based on the proposed model, which is further simplified, is developed. It is divided into three parts: (i) a feedforward control for the inlet temperature (disturbance); (ii) a simple integral action; (iii) a feedforward control to attenuate the effects of the gas velocity variations (disturbance). The proposed strategy schedules the adaptation of parameters of the control law according to the varying gas velocity. To stress the relevance of the contribution, experimental control results are presented and discussed in Section 5.

2. Control problem

2.1. Input–output description

The paper focuses on the dynamics of the simple system pictured in Fig. 1, for which the steady-state effects are easily captured.

* Corresponding author.
E-mail addresses: olivier.lepreux@ifpen.fr (O. Lepreux), yann.creff@ifpen.fr (Y. Creff), nicolas.petit@mines-paristech.fr (N. Petit).

0959-1524/$ – see front matter © 2011 Elsevier Ltd. All rights reserved.
doi:10.1016/j.jprocont.2011.10.012

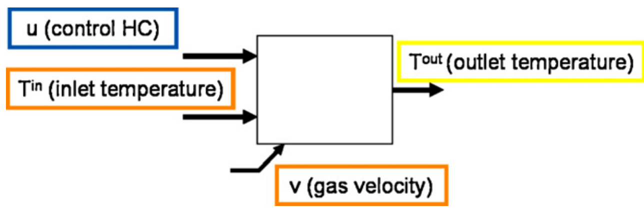

Fig. 1. DOC input–output description. The control is u, the output is T^{out}, while T^{in} and v are disturbances.

The inputs are the control variable u (control HC flow rate), the disturbance variable T^{in} (inlet temperature), and the disturbance variable v (gas velocity). *This latter disturbance defines the gas flow rate* (F), *which is of practical interest*. A straightforward relation relates the gas flow rate and the gas velocity (see below (20)). The system output is the outlet gas temperature T^{out}.

Certainly, the real picture of the DOC is more complicated, as it involves several other disturbances, among which is, in particular, an undesired reductants flow. Detailed discussions on this point can be found in [7].

2.2. Experimental setup

The experimental setup is depicted in Fig. 2 and presented in the following. The DOC is located in a Diesel engine exhaust line. The engine operating point imposes the gas velocity and the DOC inlet temperature. Two distinct configurations are used to control the reductants flow: either by an additional injector located right upstream of the turbine or by in-cylinder late post-injection. It is worth mentioning that the HCs generated by these two injection methods are different and can actually affect the overall DOC conversion efficiency [8]. This effect can be significant at some operating points. Values obtained in this paper depend on each particular tested system. Temperature is measured at three different locations and gas is analyzed upstream and downstream of the DOC by a 5-gas sensor. Presented experimental results have been obtained using two distinct engines and DOC setups. A 3-in. long and a 4-in. long platinum-based DOC have been tested.

Considering those configurations, generating a disturbance (engine emissions, T^{in}, gas velocity) independently from the others is not possible. This explains why they are not decoupled in the presented results.

The system is tested in an engine test cell, not in a vehicle. This may impact some results about heat losses.

3. Reduced model

In our model design, we desire to capture the following phenomena: the response of T^{out} to control HC (u); the response of T^{out} to inlet temperature (T^{in}); the influence of gas velocity (v). A

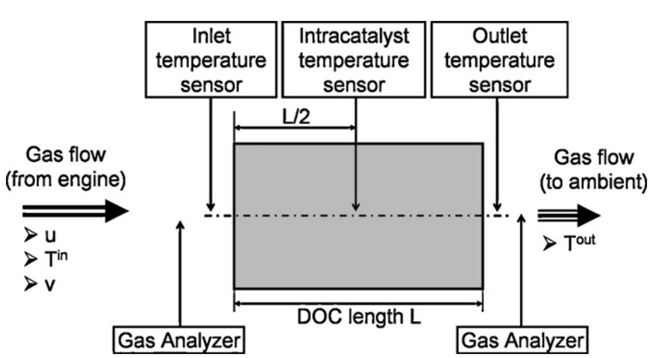

Fig. 2. Simplified overview of the DOC experimental setup.

mathematical description of the proposed reduced model is given in Section 3.1. Our goal is to get some insight into the thermal propagation phenomenon, in order to design a control law and to tune it according to the value of the gas velocity which parameterizes the model. As demonstrated by experimental validation in Section 3.2, the proposed model closely reproduces the physical observations. Interesting properties of this model will be exploited in the control strategy presented in Section 4.

3.1. Proposed reduced model

Classical models for the DOC are based on mass and energy balances for gas and "solid" phases. The presented reduced model is inferred from these. Several assumptions and steps of simplifications lead to this result. These are detailed in [7]. The main steps of simplifications are given in Appendix A.

The proposed reduced model is

$$\frac{\partial T(z,t)}{\partial t} + \vartheta(t)\frac{\partial T(z,t)}{\partial z} = \lambda(t)\frac{\partial^2 T(z,t)}{\partial z^2} + \Psi(z,u(t),v(t)) \quad (1)$$

where T is the gas temperature, $T^{\text{out}}(t) \triangleq T(L,t)$ is the system output, L is the length of the DOC, $T^{\text{in}}(t) \triangleq T(0,t)$ is a disturbance. Eq. (1) includes two parameters ϑ and λ. The parameter ϑ (in m/s) represents an *apparent speed* for the temperature, which is significantly scaled-down from the fluid speed v. The parameter λ (in m^2/s) represents an *apparent diffusion* of heat in the monolith. ϑ and λ only depend on the system disturbance v and are written as

$$\begin{cases} \vartheta(t) = \dfrac{k_2 v(t)}{k_1} \\ \lambda(t) = \dfrac{k_2 v(t)^2}{k_1^2} \end{cases} \quad (2)$$

where k_1 and k_2 are constant parameters. Ψ is a distributed source term (related to the control variable u) which is uniform over some spatial interval

$$\begin{cases} \Psi(z,u(t),v(t)) = \psi(u(t),v(t)), & 0 \le z \le L_c(v(t)) \\ \Psi(z,u(t),v(t)) = 0, & L_c(v(t)) < z \le L \end{cases} \quad (3)$$

where L_c is a piecewise affine function of the channel gas velocity v,

$$L_c(v(t)) = \min(L, a \cdot v(t) + b) \quad (4)$$

a and b being two positive constants. The source term ψ depends on v, and the control HC flow rate u according to the following relation

$$\psi(u(t),v(t)) = \frac{1}{L_c(v(t))}\eta(v(t))\frac{\Delta H_u}{\rho_g A_0 C_p}\frac{k_2}{k_1}u(t) \quad (5)$$

where ΔH_u is the heat of combustion of the control HC, C_p is the gas specific heat, A_0 is the monolith open cross-sectional area. The gas density ρ_g is assumed constant. The conversion efficiency $\eta(v)$ is mapped as a decreasing function of v only.

The steady-state gain G_u of the transfer function between the control HC flow rate and the outlet temperature is given by the following equation (steady state solution of a simple energy balance over the DOC)

$$G_u(v(t)) = \eta(v(t))\frac{\Delta H_u}{\rho_g A_0 C_p v(t)} \quad (6)$$

The model (1–6) is a linear time-varying infinite-dimensional (distributed parameter) model with distributed control (3) acting homogeneously on a reduced spatial domain defined through (4) by the disturbance variable v.

To study the proposed model involving linear operators, it can be assumed that the DOC is initially at steady state, i.e. that $T(z, 0)$

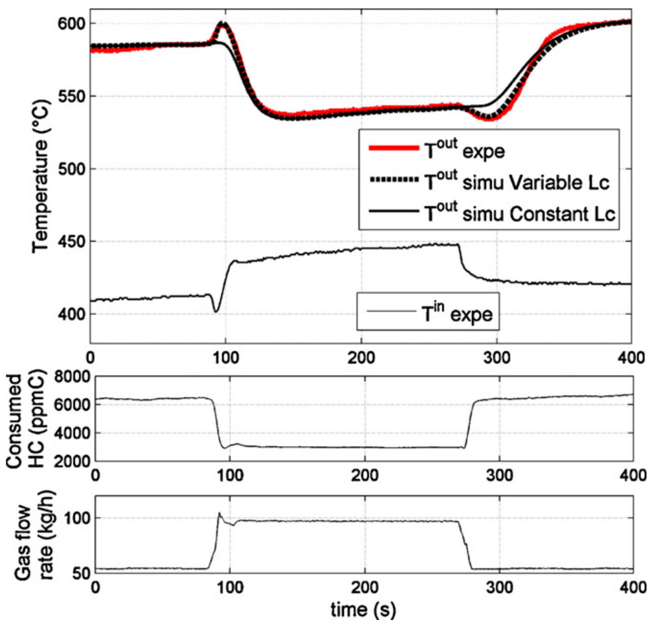

Fig. 3. Model validation under variable gas velocity conditions. The gas flow rate is an image of the gas velocity. Accounting for variable reactive length L_c reproduces the inverse response experimentally observed. Experimental and simulation data. Dead time of the HC analyzer is accounted for in this figure.

is constant. It is then correct to assume that T represents the variations of temperature about steady state instead of the (absolute) temperature itself. Therefore, from now on, the initial condition is

$$T(z,0)=0 \tag{7}$$

3.2. *Experimental validation under variable gas velocity conditions*

In the proposed model, oxidation reactions are initiated at the DOC inlet. The value of the reactive length L_c depends on the gas velocity v through (4). It is desired to investigate the relevance of this assumption. The model, simulated through a spatial finite difference scheme, is compared against an open loop experiment in Fig. 3. Physical measurements (gas flow rate, inlet temperature, inlet HC), related to the model inputs, are also plotted.

It can be noticed in Fig. 3 that a fall in the gas velocity (this fall is associated to an increase of the conversion efficiency [9]), despite an increase in HC concentration upstream of the DOC, implies an outlet temperature undershoot during a transient phase (see Fig. 3 at $t = 275$ s).

By contrast, an increase in gas velocity (associated with a fall in efficiency [9]), despite a fall in HC concentration, implies an outlet temperature overshoot during a transient phase (see Fig. 3 at $t = 90$ s).

Experimental results show that these two phenomena appear irrespective of whether the inlet temperature is rising or falling (see e.g. Section 4.2 in this paper or [7]). This is not surprising: because of the one-dimensional distributed state nature of the system, there is no direct transfer from the inlet temperature to the outlet temperature.

In Fig. 3, it appears that the temperature variations are well represented by the model. In particular, the “overshoot” and “undershoot” phenomena related to the gas velocity increase at $t = 90$ s, and decrease at $t = 275$ s are well reproduced. For comparisons, the simulation results in the case of a simpler model assuming a constant reactive length are also plotted. In this latter case, the constant value has been tuned to best fit the experimental data. Clearly, the proposed model of varying reactive length (4) outperforms it. This stresses that relating the reactive length to the gas velocity is a solution to reproduce the observed overshoot and undershoot phenomena.

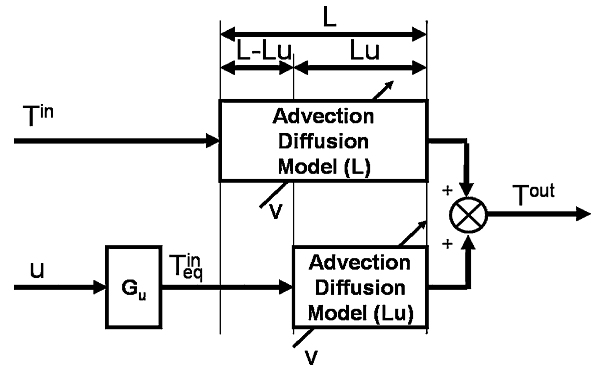

Fig. 4. Proposed control model. The HC effects can be assimilated to a front of temperature T_{eq}^{in} propagating on a fictitious length L_u. The T^{in} effect is propagating over the whole DOC length L. Propagation coefficients ($\vartheta(v(t))$ and $\lambda(v(t))$) are identical for T^{in} effects and HC effects. Hence, the difference in propagation length $(L-L_u)$ plays a keyrole for T^{in} compensation.

The reduced model for the DOC (dedicated to DPF regeneration), presented in Section 3.1, captures the main thermal effects (even transient counter-intuitive ones) observed in practice. It is needed to go further into the analysis to determine appropriate control laws. These latter are developed in the next section and presented together with the experimental results in Section 5.

4. Control strategy

In this section, the proposed model (1–6) is used for the development of the control law. This is done in two steps. In Section 4.1, the reactive length L_c is *preliminarily assumed constant* (independent of v). A control strategy dedicated to T^{in} disturbance rejection is presented. In Section 4.2, the control law is adapted to account for the dependency of L_c upon v. Finally, the last part of the section sums up the proposed control solution.

4.1. *Control strategy for a constant reactive length*

In this subsection, it is assumed that the reactive length L_c is constant (not depending on v), i.e. $a = 0$ in (4).

4.1.1. *Proposed control model*

In the proposed control model, the effects of the control u and the effects of the inlet temperature T^{in} can be decoupled. This is pictured in Fig. 4.

On one hand, the control variable u of the reduced model can be turned into a temperature boundary condition. The system can be approximated by an advection-diffusion system having a reduced length $L_u(v(t))$ (in practice related to $L-L_c(v(t))$):

$$\frac{\partial T(z,t)}{\partial t}+\vartheta(t)\frac{\partial T(z,t)}{\partial z}=\lambda(t)\frac{\partial^2 T(z,t)}{\partial z^2} \tag{8}$$

where the left-side boundary condition depends on the control u and writes $T(z=L-L_u(v(t)),t)=T_{eq}^{in}(t)=G_u(v(t))u(t)$, and the right-side boundary condition $\frac{\partial T}{\partial z}(z=L,t)=0$. The domain considered for z is $z\in[L-L_u(v(t)),L]$: it depends on the disturbance $v(t)$.

On the other hand, using the linearity of (1), the inlet temperature is taken into account through the response to its boundary condition while zeroing the source term. The inlet temperature propagation is described by a standard advection-diffusion

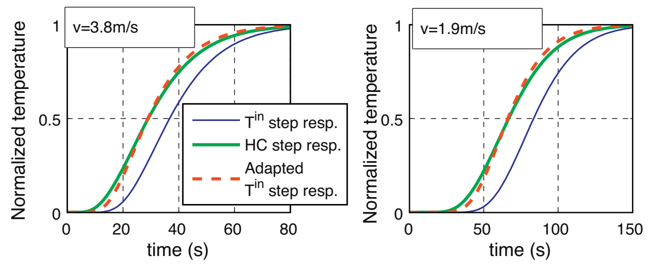

Fig. 5. Normalized step response approximation under various operating conditions. Comparison between HC step response (distributed input of the reduced model), T^{in} step response (boundary input of the reduced model), and T_{eq}^{in} step response using an adapted value of the length (equivalent boundary input of the reduced model). Simulation results obtained from a spatial discretization of (1).

system of the form (8), over a constant length L ($z \in [0, L]$) and T^{in} as left-side boundary condition: $T(z=0, t) = T^{in}(t)$.

Step responses for these two systems are plotted in Fig. 5. It can be observed that the HC step response, obtained with a system having a length L is very similar to the T^{in} response of the system translated in time. Further, it is shown that the overall shape of the HC step response, corresponding to a distributed input (computed with (1) and $T^{in} = 0$), is very similar to the inlet temperature step response, corresponding to a boundary input (computed using (1), $\psi = 0$, and $z = L$). This similarity supports that it is possible to approximate the HC step response by a boundary input step response at the expense of an alternative identification procedure (note that, for easier comparisons, responses are normalized).

It is shown in Fig. 5 that it suffices to fictitiously adapt the DOC length in the model (1) and to use its boundary input with $\Psi = 0$, to get responses very similar to the ones obtained using its distributed input Ψ and the full length L. *In other words, generating heat with HC is quite equivalent to propagating an inlet temperature condition through a DOC having a shorter length* L_u [7]. This idea focuses on the heat propagation along the DOC rather than on the way heat is generated. Note that this fictitious "transport" length L_u, carefully tuned to match experimental data, need not equal the "non-reactive" length (i.e. $L - L_c$). In typical cases, everything behaves as if the source were located at about half the reactive length L_c. To precisely get the two viewpoints in accordance, a numerical identification is performed. This yields an affine relation between L_u and v. The two corresponding parameters are denoted a_{L_u} and b_{L_u}.

In summary, gathering the two discussed effects, a schematic view of the T^{in} effects and the HC effects is presented in Fig. 4. The effects of the HC flow rate u can be assimilated to a temperature T_{eq}^{in} propagating on a fictitious length L_u, which is shorter than the DOC real length. Besides, T^{in} is propagating over the whole DOC length L. Consequently, the inlet temperature effects are slower than the HC effects. Both sub-subsystems use the advection-diffusion equation to describe propagation. Although variable, v is identical in both sub-systems, and, in particular, does not depend on z. This interesting property allows us to decouple the T^{in} effects and the HC effects. In both sub-systems, propagation coefficients (ϑ and λ) are identical (and depend on v). Altogether, the constituted control model consists of the discussed two sub-models, the outputs of which are added up to yield the model output.

These submodels are exploited in the control strategy for disturbance rejection and feedback compensation. To this aim, it is shown in the next part how delays can be computed from these models.

4.1.2. Delay evolution under variable gas velocity conditions

Variations of the gas velocity (v), that have been ignored so far, are now accounted for under the form of a traveling time for the thermal propagation phenomena. This time $\delta(t)$ will be used in the control design.

Consider the delay $\delta(t)$ defined by $T(z, t) = T(z - z_p, t - \delta(t))$ where z_p represents the considered length of propagation. It can be shown (see e.g. [7]) that the delay evolution satisfies the following implicit equation, in which $\delta(t)$ is unknown

$$z_p = \int_{t-\delta(t)}^{t} \vartheta(w)dw \tag{9}$$

This implicit equation will be used to describe the evolution of thermal phenomena and, in particular, to synchronize the control action with the measured disturbance.

To simplify the calculation, *it has been assumed that the approximations that have led to the reduced model hold when v depends on time.* Hence, $\vartheta(t) = k_2 v(t)/k_1$ and $\lambda(t) = k_2 v(t)^2/k_1^2$ are now considered. The advection-diffusion equation (8) allows, under some conditions, to separate the propagation effect from the diffusion phenomenon. Following several calculations given in [10], this separation is highlighted by invoking the following change of variables $w(\zeta, \tau) = T(z, t)$, with $\zeta = z - \int_0^t \vartheta(s)ds$ and $\tau = \int_0^t \lambda(s)ds$ (see [7]). Then, Eq. (8) simply leads to the heat equation $\partial w/\partial\tau = \partial^2 w/\partial\zeta^2$. This transformation can also be performed under variable conditions because the advection-diffusion coefficients λ and ϑ only depend on the time variable t through v (not on z). In these coordinates, it is possible to study the propagation on a system having an infinite length. In this infinite-length system, the boundary conditions are located at $\zeta = \pm\infty$ in the (ζ, τ)-coordinates or at $z = \pm\infty$ in the (z, t)-coordinates. It is considered that the boundaries are "far" from the studied phenomena (relatively to diffusion effects). Then, under these conditions, it is possible to solve (9) with respect to the propagation delay $\delta(t)$. The reader can refer to [7] for more details.

4.1.3. Feedforward control strategy for a constant reactive length

It is possible to compensate for effects of T^{in} by synchronization with delayed effects of u. As pictured in Fig. 4, the synchronization between T^{in} and u must be considered on the first part of the DOC for the length difference $L - L_u$. Hence, from the advection-diffusion model viewpoint, the delay $\delta_{FF}(t)$ to synchronize the inlet temperature variations with the control HC variations is simply given by the implicit equation, in which $\delta_{FF}(t)$ is unknown and ϑ represents an apparent propagation speed[1]:

$$L - L_u = \int_{t-\delta_{FF}(t)}^{t} \vartheta(w)dw \tag{10}$$

Finally, a feedforward compensation block for the T^{in} disturbance can be simply based on a delay operator applying a delay value of $\delta_{FF}(t)$

$$u_{FF}(t) = \frac{1}{G_u^{dyn}(t)} T^{in}(t - \delta_{FF}(t)) \tag{11}$$

where u_{FF} is the feedforward HC flow to deliver in order to reject T^{in} variations, and where G_u^{dyn} is a dynamically updated version of G_u that will be detailed in Section 4.2.

4.1.4. Feedback control

As detailed before, control HC effects for a catalyst length L are equivalent to boundary temperature effects for a catalyst length

[1] Note that analytic responses to HC and T^{in} have been compared in Fig. 5 (using the reduced model). *It has been shown that inlet temperature effects are slower than HC effects. It is then theoretically possible to compensate totally for these variations.* In the advection-diffusion system representation, this ensures that the equivalent propagation length L_u is smaller than the full DOC length L. In other words, it ensures that the delay $\delta_{FF}(t)$ is positive or null, so that the control law can be applied.

L_u. A variation of HC is interpreted as a boundary condition $T_{eq}^{in}(t)$ of system (8) over a propagation length L_u. Applying results of Section 4.1.2, HC response time calculation can be based on the evaluation of the following implicit equation in which δ_{FB} is the unknown:

$$L_u = \int_{t-\delta_{FB}(t)}^{t} \vartheta(\tau)d\tau \tag{12}$$

For an HC step input, δ_{FB} is approximately the time at which the outlet temperature reaches half its steady-state value.

As will be developed in Section 4.2, in practice, DOC outlet temperature cannot be perfectly controlled due to changes (slips) of the reactive zone during gas velocity variations. Induced overshoot and undershoot phenomena have been discussed in Section 3.2. Typically, for a 4-in. long DOC, practical achievable performance is about ±15 °C. This observation is a big concern because this result is close to the performance requested for real applications. Therefore, the feedback control in this zone cannot be totally turned off (as would be done for example by a usually considered deadzone strategy) but it has to be loosely tuned. Typically, in this zone, it is not possible to use a classic feedback control law because error to setpoint is related to hardly compensable disturbance effects.

To compensate for steady-state errors, a simple integral action is used. To obtain the results presented in this paper (see Section 5), the integral time is empirically set to

$$\tau_i = 2 \cdot \delta_{FB} \tag{13}$$

This means that, for a given gas velocity, the integral time is approximately set equal to the duration of the HC effect. Finally, the feedback action of the controller is given by a simple integral term

$$u_{FB}(t) = \frac{1}{G_u^{dyn}(t)} \int_0^t \frac{1}{\tau_i(w)} \left(T^{sp}(w) - T^{out}(w)\right) dw \tag{14}$$

where T^{sp} is the outlet temperature setpoint.

Note that adaptations of this law can be used for large setpoint variations [11].

4.2. Generalization of the control law for variable gas velocity

In the previous subsection, the dependence of L_c upon v, stated by (4), has been ignored. In this subsection, it is shown how the control law previously developed can be adapted to account for the overshoot and undershoot phenomena, i.e. for a variable reactive length L_c.

The overshoot phenomenon stems from the combination of heat storage and under-actuation effects, on a reactive length that is defined by a disturbance, namely the gas velocity. *We refer the reader interested by the origins of the overshoot to* [9,7], where a simple advection model is used to illustrate this point. The presented analytic study shows that an increase in the reactive length causes an overshoot. An analytic control trajectory to limit the overshoot is proposed in [9]: when the gas velocity increases, the static gain is transiently decreased in order to limit the coming overshoot. This overshoot compensation induces an undershoot.

In the following, a specific feedforward control law that closely imitates this approach is presented and open loop experiments are reported.

An easy-to-implement dynamic gain adaptation is used, based on the time derivative of the gas velocity. A filtered derivative of the speed $v(t)$ is computed. The filter is a first order filter with time constant τ_B. The filtered derivative is normalized with the current value of the gas velocity, and multiplied by a gain K_B to give a correction term X. The gain G_u^{dyn} used is given by $G_u^{dyn} = G_u/(1-X)$. According to this relation, a rise (resp. decrease) of $v(t)$ induces a rise (resp. decrease) of X: the value G_u^{dyn} of the gain is then larger (resp. smaller) than the values of the static gain G_u. Accordingly, the control u is less (resp. more) than what is required to keep T^{out} constant. While $v(t)$ stabilizes to a new constant value, its derivative tends to 0. Then, X tends toward 0 and, as G_u^{dyn} tends toward G_u, the control u takes the value that is required to reach T^{out} setpoint. In details,

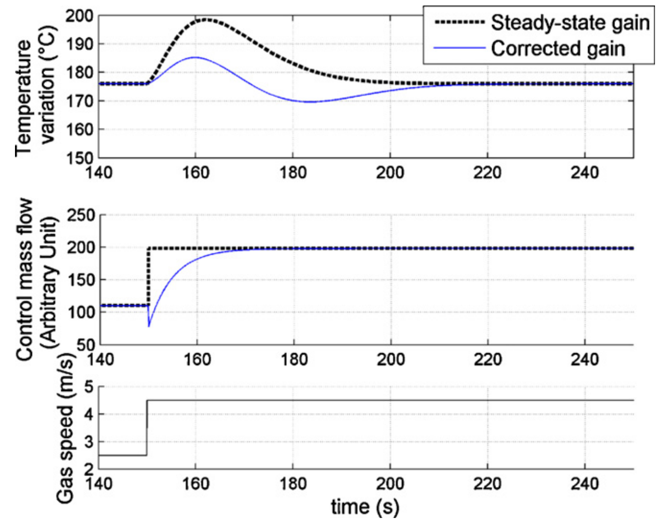

Fig. 6. Illustration of overshoot compensation based on gas velocity derivative. Simulation data.

$$\frac{1}{G_u^{dyn}(v(t))} = \frac{1-X(t)}{G_u(v(t))} \tag{15}$$

where $X(t)$ is given by $Y(t)/v(t)$, $Y(t)$ corresponds to the inverse Laplace transform of $\hat{Y}(s)$ given by

$$\hat{Y}(s) = \frac{K_B s}{1+\tau_B s}\hat{v}^{sat} \tag{16}$$

and v^{sat} is the saturated value of the current gas velocity. This saturation corresponds to the saturation of the length L_c in (4).

K_B is a tuning parameter corresponding to the compensation strength. The greater K_B is, the more the control u is adapted during gas velocity transients. If set too high, this parameter will favor delayed side effects. Besides, τ_B is a tuning parameter corresponding to a time during which the compensation acts after a gas velocity variation. Referring to [7], it should be theoretically adapted to the current variation of L_c. However, in practice, this extra tuning is not needed since the correction is already quite efficient with constant parameter values.

The main advantage of this method is that it is extremely simple to implement. It is also interesting to notice that the use of a filtered derivative ensures a good robustness regarding the noise of the air flow sensor measurement which is used in the computation of the gas velocity.

The behavior of the law is illustrated in Fig. 6 by a simulation, carried out with the model (19).

In this simulation, the open loop control strategy acts as soon as the gas velocity variation is detected. The control variable significantly differs from the case of the static strategy. One can see that the reduction of the overshoot magnitude is indeed effective. However, the consequence of this action is a delayed temperature undershoot. The behavior is confirmed by the open loop experiment presented in Fig. 7. This is an important result for control application since undershooting does not increase the risks of DPF runaway. However, overshoot compensation is limited: it is usually better to allow a small overshoot in order to prevent large delayed undershooting.

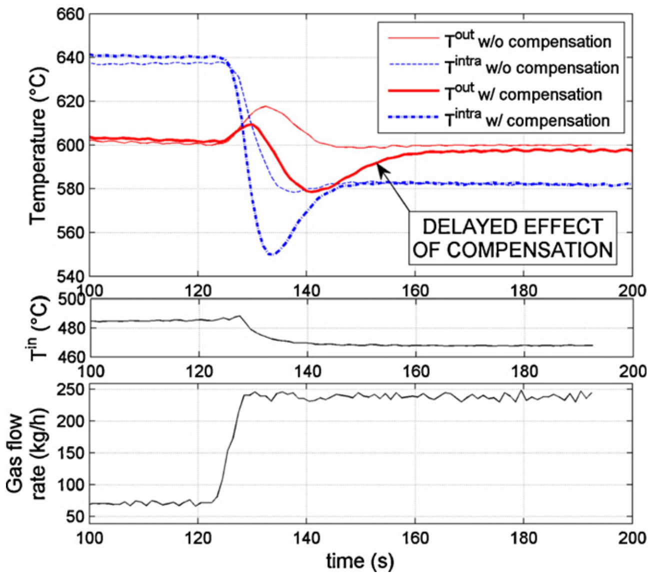

Fig. 7. Catalyst undergoes a large increase in the gas velocity at $t \approx 125$ s. The gas flow rate is an image of the gas velocity. Without compensation, HC flow is adapted to keep a constant inlet HC concentration. With compensation, HC flow is temporarily reduced when the gas velocity variation is detected. With compensation, the overshoot is attenuated but still present. Moreover, when compensating, a delayed undershoot appears consequently to the transient drop in heat supply. T^{in} is plotted for information but has no consequence on the described phenomenon. Experimental data obtained with a 4-in. long DOC.

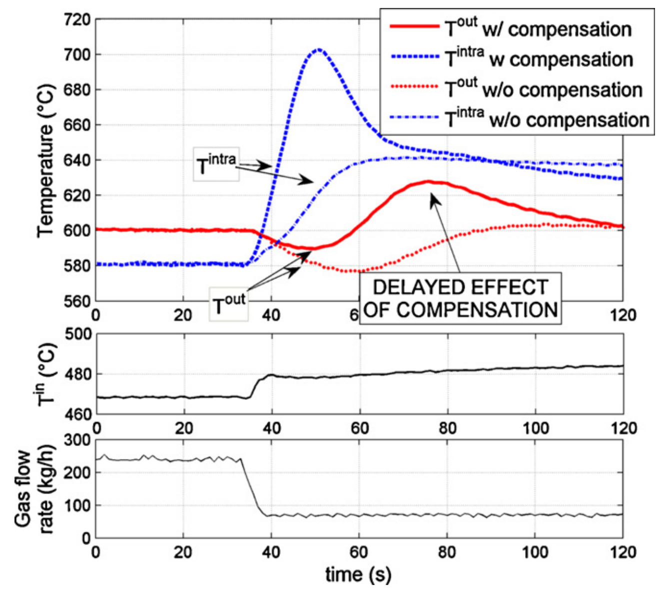

Fig. 8. Catalyst undergoes a large decrease in the gas velocity at $t \approx 35$ s. The gas flow rate is an image of the gas velocity. When compensating the undershoot by a more-than-steady-state HC flow, a delayed overshoot appears consequently to the transient excess in heat supply. T^{in} is plotted for information but has no consequence on the described phenomenon. Experimental data obtained with a 4-in. long DOC.

A similar experiment has been carried out in the case of an undershoot, as pictured in Fig. 8. Although it generates no particular risk of DPF damage, this variation is problematic for DPF regeneration. It increases the time required to oxidize the trapped soot and, in turn, also increases the fuel consumption. However, it is desired to show that it cannot be compensated without side effects. As in the case of the overshoot, it is shown that the undershoot is not totally compensated by the above mentioned strategy. It is only reduced. It is worth noticing that this action causes a delayed temperature overshoot (as can be noticed in Fig. 8).

This delayed overshoot is caused by the "additional" quantity of HC injected during the gas velocity drop. Time duration between the pulse (and the gas velocity variation) and the delayed overshoot is related to one-dimensional effects of the system. Intuitively, the pulse acts in a distributed way on the reactive length L_c, which has been reduced during the transient state. Therefore, the pulse has no direct action on this gap: it always acts upstream. In fact, considering the involved time scales, the pulse effects and the supply gap effects are combined together and smoothed by diffusion effects. This explains why the undershoot is attenuated by the pulse. For the reasons mentioned previously, from a practical viewpoint, this delayed overshoot is not suitable. It is not easy to "re-compensate" for it, as this would imply an oscillatory highly delayed control. Consequently, the undershoot must be carefully compensated for.

As has been demonstrated, the proposed feedforward strategy for the gas velocity disturbance is simple and effective. In practice, the temperature overshoot (and undershoot), which is caused by an increase (and a decrease) in the gas velocity, should not be totally compensated for. As a consequence, the achievable performance for the DOC outlet temperature control is limited. Depending on the tested DOC device, the expected range of performance would commonly not be better than ±10 °C to ±20 °C (or even worse)—see [9,7] for more details.

4.3. Summary of control problem and solution

The physical analysis and simplified modeling of the thermal phenomena detailed in the previous sections are here briefly summed up. Following along these lines, the control problem can be specified in the scheme presented in Fig. 9. Referring to this figure, the outlet temperature is the output variable. The control HC

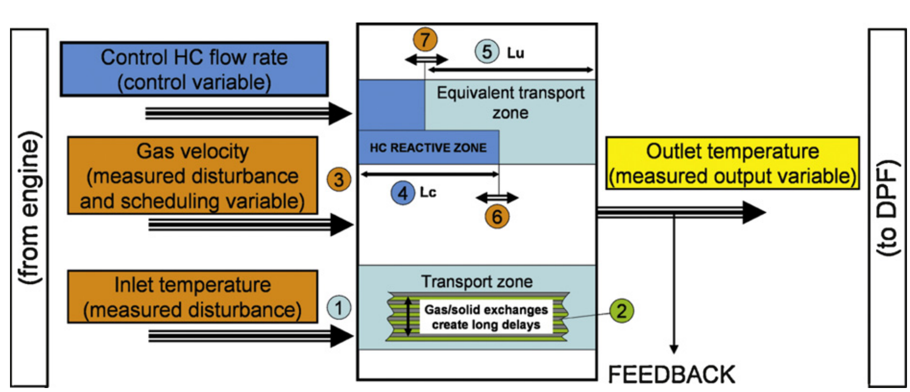

Fig. 9. Control problem viewpoint after analysis of the thermal phenomena.

flow rate u is the control variable. The inlet temperature variations (mark 1) are propagating through the DOC, creating long delays due to the gas/solid heat exchange (mark 2). The inlet temperature is regarded as a disturbance. The delay values are strongly related to the gas velocity (mark 3). For the delays, the gas velocity (mark 3) is regarded as a scheduling variable. The control HC flow is oxidized on a reactive length L_c (mark 4). The control HC flow rate is regarded as a distributed control variable. Alternatively, it can be regarded as a boundary control variable equivalent to a temperature variation for a catalyst having an equivalent transport length L_u (mark 5). Temperature rise corresponding to the control HC flow is strongly related to the gas velocity (mark 3), which is, once again, regarded as a scheduling variable. The gas velocity (mark 3) is not only a scheduling variable. When varying, it makes the reactive length – and the equivalent transport zone – vary (marks 6 and 7). Then, it creates temperature disturbances inside the DOC. This is why it is also regarded as a disturbance. The conversion efficiency is taken into account explicitly in the injection calculation of the control input by (5).

From the previous description, a control strategy can be proposed. It is implemented in three parts as schematized in Fig. 10. First, a feedforward control law, designed to compensate the measured inlet temperature disturbances, is given by (10) and (11) (block (1) in Fig. 10). Then, a simple integral effect is introduced by (12)–(14) (block (2) in Fig. 10). Finally, a feedforward strategy accounting for the gas velocity disturbance is given by (15) and (16) (block (3) in Fig. 10) under the form of an adaptation of parameter using available gas velocity information.

The overall controller has few parameters. The most important ones are related to physical quantities (k_1,k_2,a_{Lu},b_{Lu}). They are obtained by identification through only few experiments, or are directly measured (η is given by a table). Controller-specific parameters (K_B,τ_B) require little tuning effort.

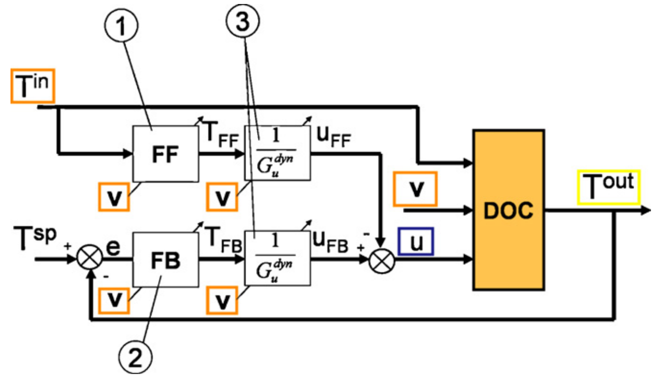

Fig. 10. Advanced controller overview. Block (1) corresponds to the feedforward control related to the inlet temperature. Block (2) corresponds to the feedback control. Blocks (3) correspond to the feedforward control related to the gas velocity. T^{in} and v are the measured inputs. T^{out} is the measured output.

5. Experimental results

5.1. Experimental results

In this section, three practical cases using the temperature controller are presented. The first experimental result corresponds to a large drop in the gas velocity, which is a difficult situation to handle. The second result illustrates the controller ability to deal with large and dynamic gas velocity transients. The third experimental result corresponds to the urban part of the normalized European driving cycle (NEDC [1]), which is the most difficult part of the NEDC in terms of control application (lowest speeds, largest delays).

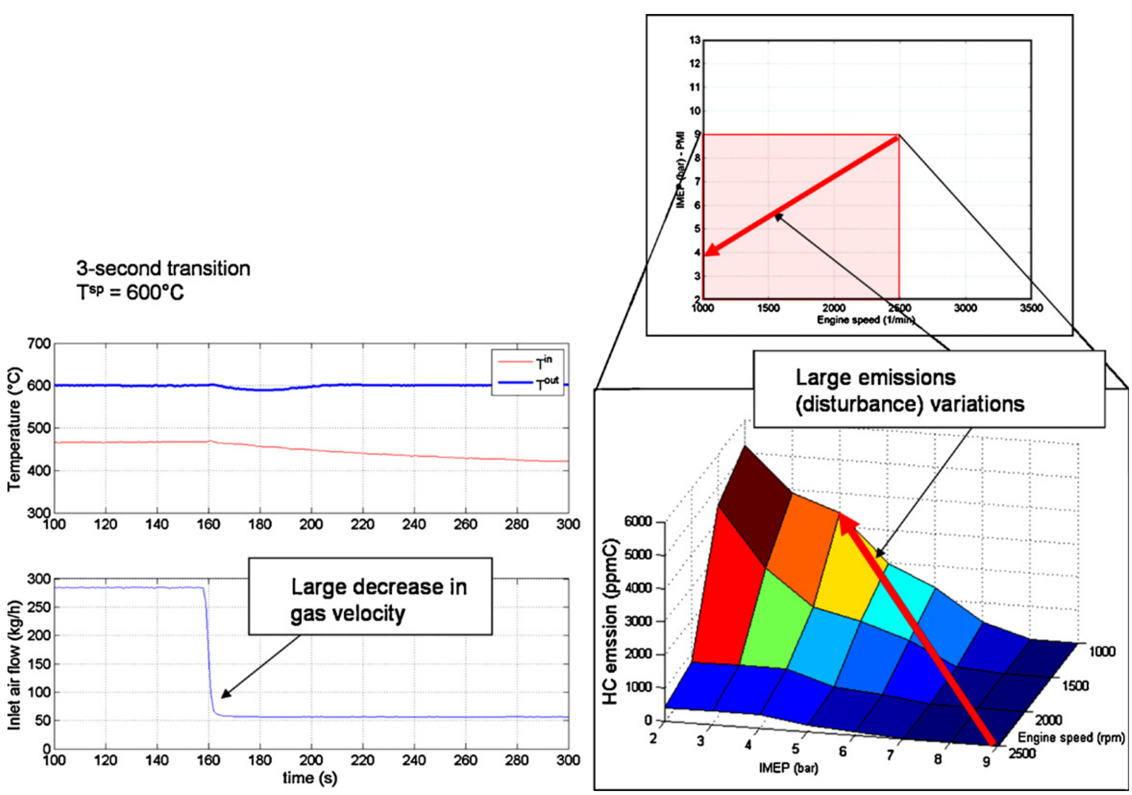

Fig. 11. Results of T^{out} control during a drop in the gas velocity. The gas flow rate is an image of the gas velocity. The DOC outlet temperature error remains within ±11 °C. IMEP (indicative mean effective pressure) is an image of the engine load. Experimental data obtained with a 3-in. long DOC.

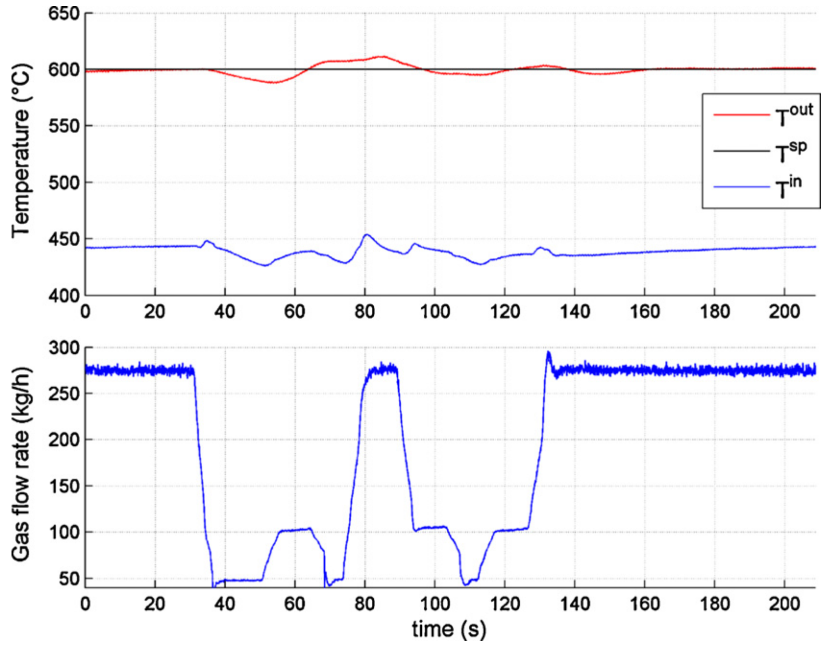

Fig. 12. Results of T^{out} control during large gas velocity variations. The gas flow rate is an image of the gas velocity. The DOC outlet temperature error remains within ±10 °C. Experimental data obtained with a 4-in. long DOC.

5.1.1. Scenario 1: large gas velocity variations

This situation is close to a drop-to-idle situation. It corresponds to a realistic and problematic case of interest. This situation typically happens when a vehicle switches from motorway driving to urban driving. Once the regeneration process has started, in order to save fuel, regeneration time and catalyst wear, it is better to continue the regeneration process.

Drop-to-idle tests are among the most difficult situations to control. Control difficulties in this kind of situations are that (i) large drop in gas velocity implies large non-compensable temperature effects (undershoot); (ii) large drop in gas velocity implies large delay variation. Also, the final delay (i.e. the delay after the variation) is very large; (iii) the disturbance reductants flow is varying to a large extent.

Dealing with large gas velocity increase is easier than dealing with gas velocity decrease because the final delays (delays after the variation) are small. Small-delay situations can be efficiently treated by feedback control. Also, the disturbance reductants flow rate is almost zero in this situation.

Note that the presented case does not exactly correspond to an "idle" point. This is because it is difficult to keep a reasonable DOC inlet temperature level. The corresponding level of disturbance reductants is high, and it varies so that there is a real need to estimate them. Theoretical estimation is beyond the scope of this work. Empirical estimation is difficult because of the emissions variability. On low-load low-speed engine operating points, disturbance reductants cause inlet-to-outlet steady-state temperature rise as high as 100 °C with high variability. A little time has been spent on this point with this setup. It has been preferred to focus on another setup to obtain the results presented in the next scenarios.

In Fig. 11, the inlet gas flow rate sensor measurement is represented. At $t \approx 160$ s, the engine operating point is changed in a 3-s transition from 2500 rpm-9 b (IMEP) to 1000 rpm-4 b (IMEP). From this time the inlet temperature continuously decreases in a medium range. One can report to Fig. 11 to get the corresponding steady-state disturbance HC emissions levels.

5.1.2. Scenario 2: experimental full range cycle

The situation presented in Fig. 12 corresponds to large and dynamic gas velocity transients. It corresponds to an aggressive driving situation.

This test stresses the controller ability to deal with large and frequent gas velocity variations. These variations are higher and more frequent than those taking place during a normalized European driving cycle. Then, this situation might seem more difficult to control. However, this is not the case, because in this situation the gas velocity often increases to high values. When these values are reached, the delay becomes very small and the presented feedback control is very efficient. Hence, these high gas velocity values regularly "reset" the history in the DOC, which can be viewed as a finite memory system, as well as feedforward correction errors. This is described by the general formula (9) in which δ is small when ϑ is high.

5.1.3. Scenario 3: experimental urban cycle

The test presented in this section corresponds to the urban part of the normalized European driving cycle (NEDC). It is composed of four ECE driving cycles. It is usually run when the engine is cold to test engine pollutant emission levels. However, DPF regeneration phases are started with warm engine. So, the presented test is run when the engine is already warm.

Although this test (presented in Fig. 13) is less aggressive than the full range cycle presented in Scenario 2 for example, it represents one of the most difficult situation to control, together with the drop-to-idle test. In fact, operating points are continuously in difficult to control zones, which gather the four following difficulties: (i) zones where delays vary on the sensitive part of the curve as pictured in Fig. 14; (ii) zones where the length of combustion is strongly impacted, leading to large and frequent non-compensable disturbance effects; (iii) zones where the inlet temperature largely varies; (iv) zones where the disturbance reductants flow rate largely varies. Hence, it is not more difficult to control larger and more frequent variations. Then, this experiment is considered particularly relevant to test the controller performance.

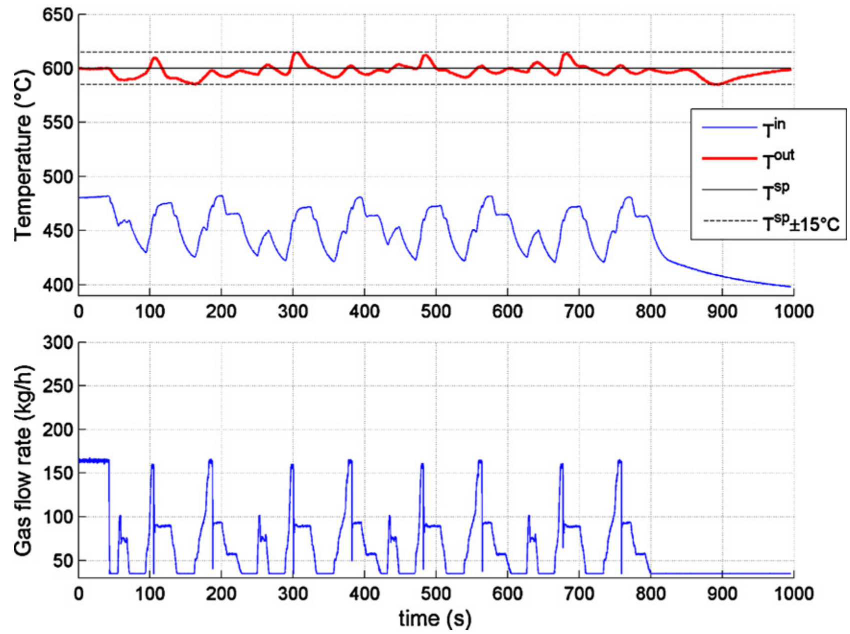

Fig. 13. Results of T^{out} control for the urban part of the NEDC driving cycle. The DOC outlet temperature error remains within ±15 °C. Experimental data obtained with a 4-in. long DOC.

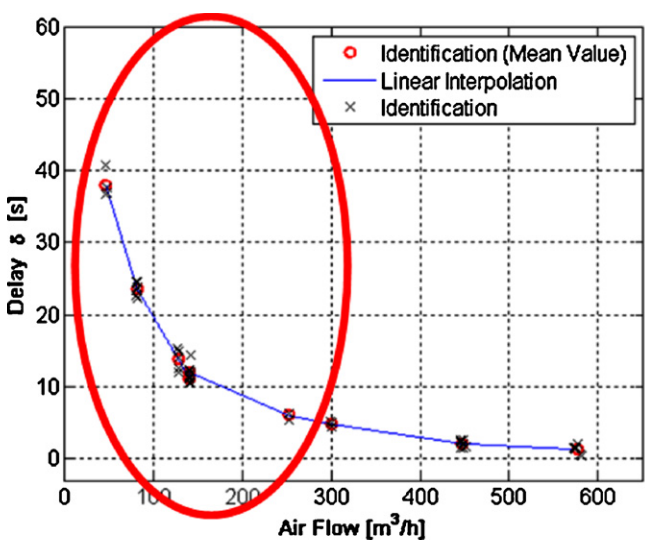

Fig. 14. Illustration of delays involved during an urban cycle. Experimental step test data – for control model calibration – are identified to a first order plus delay model using a least mean-square algorithm.

5.2. Conclusions

The proposed control strategy has been tested on an engine testbench. Experimental results are close to the best achievable performance (see Section 4.2) in particularly difficult situations: urban driving cycle and large gas velocity transients. In particular, performance on the urban part of the NEDC cycle obtained with a 4-in. long DOC is ±15 °C about the setpoint value.

6. Conclusion

In this article, the problem of the thermal control of a DOC (diesel oxidation catalyst) as used in aftertreatment systems of diesel vehicles has been studied. It has been stressed that the one-dimensional distributed nature of the DOC causes long and largely varying time responses of the outlet temperature (measured output variable) to HC flow (control variable) and inlet temperature (measured disturbance). A first contribution of the paper is the control model of Section 4.1.1 (Fig. 4), describing the response of the system to these two input signals. Then, it has been shown that a model-based approach successfully addresses the problem of DOC outlet temperature control despite large and frequent disturbances. The controller detailed in Section 4.3 and pictured in Fig. 10 is the second contribution of the article. Conveniently, it has few parameters and requires light calibration effort. It accounts for the main physical observations that can affect the control performance. The proposed strategy is mainly dedicated to disturbances rejection. It synchronizes the HC flow (control variable) to the inlet temperature (measured disturbance). It is completed by an integral effect feedback control strategy, based on the delay evaluation from the proposed control model. Further, an additional feedforward control strategy partially compensates for effects related to gas velocity variations (measured disturbance). Altogether, the solution proves to be efficient on an engine testbench. It leads to a control performance among the best practically achievable results: for the tested 4-in. long DOC, the outlet temperature can be kept within ±15 °C of the setpoint on the urban part of the normalized European driving cycle (NEDC) [1].

Appendix A. Main steps leading to the proposed (advection-diffusion) model

This appendix gives some insight on how the model (1) can be derived. A model describing two phases exchanging energy through two hyperbolic equations is presented. Main steps leading to its approximation by a parabolic advection-diffusion model are presented. To obtain this model, a low-order series expansion of the partial differential equation is performed.

A.1. Two-phase reduced model

Numerous models have been used and improved since the 1960s for oxidation catalysts. Following the review of [5], several key simplifying assumptions are usually considered. A model for the DOC can be written as (17). It is obtained from energy balances for the gas and the solid phases. Corresponding assumptions will be described hereafter.

$$\begin{cases} \underbrace{\varepsilon\rho_g Cp\frac{\partial T}{\partial t}(z,t)}_{\text{Gas storage term}} + \underbrace{\frac{F(t)}{A_{cell}}Cp\frac{\partial T}{\partial z}(z,t)}_{\text{Advection term}} = \underbrace{-h_g G_a\left(T(z,t)-T_s(z,t)\right)}_{\text{Convection term}} \\ \underbrace{(1-\varepsilon)\rho_s Cp_s\frac{\partial T_s}{\partial t}(z,t)}_{\text{Solid storage term}} = \underbrace{h_g G_a\left(T(z,t)-T_s(z,t)\right)}_{\text{Convection term}} + \underbrace{G_{ca}\sum_{j=1}^{NM} R_j(t)\cdot h_j}_{\text{Heat source term}} \end{cases} \tag{17}$$

T and T_s are the gas and monolith temperature, ρ_g and ρ_s are the gas and monolith densities, Cp and Cp_s are the specific heat of the gas and of the monolith, ε is the ratio of gas volume to total volume (void ratio), A_{cell} is the mean cell cross-sectional area (wall and channel), h_g is the convective heat transfer coefficient between gas and solid, G_a is the geometric surface area-to-volume ratio, G_{ca} is the catalytic surface area-to-volume ratio, R_j is the rate of reaction of species j, h_j is the enthalpy of chemical species j, and NM is the number of considered species. For more details on these variables, the reader can refer to [5].

In the proposed model of Section 3.1 (dedicated to DPF regeneration), several assumptions are made: the DOC is supposed to be thermally isolated and heat losses to the surroundings are neglected, axial diffusion in the fluid and solid phases can be neglected, the Nusselt and Sherwood numbers [12] (respectively, included in h_g and R_j) can be assumed constant. Further, in the proposed model, the source term is lumped into a function Ψ defined by

$$\begin{cases} \Psi(z,u(t),v(t)) = \psi(u(t),v(t)), & 0\le z\le L_c(v(t)) \\ \Psi(z,u(t),v(t)) = 0, & L_c(v(t)) < z \le L \end{cases} \tag{18}$$

Exothermic reactions are lumped into a single source term, disturbance reductants are considered separately from this term, the source term is independent of catalyst temperature, chemical and thermal dynamics are decoupled, $\Psi(z,u(t),v(t))$ can be described by a uniform profile as stated by (18), the reactive length L_c can be modeled as a function of variable v only, and temperature rise can be expressed as a function of the gas velocity only. More details on these assumptions can be found in [7]. Then, the model (17) can be rewritten as

$$\begin{cases} \frac{\partial T}{\partial t}(z,t) + v(t)\frac{\partial T}{\partial z}(z,t) = -k_1(T(z,t)-T_s(z,t)) \\ \frac{\partial T_s}{\partial t}(z,t) = k_2(T(z,t)-T_s(z,t)) + \Psi(z,u(t),v(t)) \end{cases} \tag{19}$$

where parameters can be related to the physical parameters in (17) with

$$\begin{cases} k_1 = \dfrac{h_g G_a}{\varepsilon\rho_g Cp} \\ k_2 = \dfrac{h_g G_a}{(1-\varepsilon)\rho_s Cp_s} \\ v(t) = \dfrac{F(t)}{\rho_g\varepsilon A_{cell}} = \dfrac{F(t)}{\rho_g A_0} \end{cases} \tag{20}$$

A.2. Advection-diffusion equation approximation

In (19), neglecting the gas thermal storage term $\partial T/\partial t$ (which is a reasonable assumption), derivating the first equation with respect to t, and substituting T_s and $\partial T_s/\partial t$ in the second equation leads to (not considering the source term here)

$$\frac{\partial T(z,t)}{\partial t} + \vartheta\frac{\partial T(z,t)}{\partial z} + \frac{\lambda}{\vartheta}\frac{\partial^2 T(z,t)}{\partial t\partial z} = 0 \tag{21}$$

Following [13], T is expanded in the series (when $\varepsilon \triangleq \lambda/\vartheta = v/k_1$ is small) $T = T_0 + \varepsilon T_\varepsilon + \varepsilon^2 T_{\varepsilon^2} + \ldots$, where T_0 is the solution of the following advection equation

$$\frac{\partial T_0(z,t)}{\partial t} + \vartheta\frac{\partial T_0(z,t)}{\partial z} = 0 \tag{22}$$

On one hand, expanding solutions of T in ε for (21) leads to

$$\varepsilon\frac{\partial^2 T_0}{\partial t\partial z} + \varepsilon\frac{\partial T_\varepsilon}{\partial t} + \vartheta\varepsilon\frac{\partial T_\varepsilon}{\partial z} + \varepsilon^2\frac{\partial^2 T_\varepsilon}{\partial t\partial z} + \ldots = 0$$

On the other hand, expanding solutions of T in ε for the advection-diffusion equation $(\partial T(z,t)/\partial t) + \vartheta(\partial T(z,t)/\partial z) = \lambda(\partial^2 T(z,t)/\partial z^2)$ leads to

$$\varepsilon\frac{\partial^2 T_0}{\partial t\partial z} + \varepsilon\frac{\partial T_\varepsilon}{\partial t} + \vartheta\varepsilon\frac{\partial T_\varepsilon}{\partial z} - \varepsilon^2\vartheta\frac{\partial^2 T_\varepsilon}{\partial z^2} + \ldots = 0$$

So, expanding solutions of T in ε for (21) and for the advection-diffusion equation leads to the same equations up to order 1 in ε, i.e. T_0 and T_ε are the same in both cases. In this way they are similar: their asymptotic expansions are equal up to order 1 (included) (see [7,13] for further calculation details). Considering these results yields the model (1).

Another way to proceed to highlight the relationship between the two partial differential equations is as follows. Successively, one can differentiate the simple cascade of partial differential equations obtained for each term $T_0, T_\varepsilon, \ldots$ by matching powers of ε. A summation of those differential relations makes the sought-after diffusion equation appear, along with a (distributed) source term, taking the form of a series, whose magnitude is ε^3, which, again, suggests that the two equations are indeed closely related.

References

[1] Ecopoint Inc., DieselNet, Available online: http://www.dieselnet.com/.
[2] E. Bisset, Mathematical model of the thermal regeneration of a wall-flow monolith diesel particulate filter, Chem. Eng. Sci. 39 (1984) 1232–1244.
[3] L. Achour, Dynamique et contrôle de la régénération d'un filtre à particules diesel, Ph.D. Thesis, École des Mines de Paris—MINES ParisTech (2001).
[4] G. Koltsakis, A. Stamatelos, Catalytic automotive exhaust aftertreatment, Prog. Energy Combust. Sci. 23 (1997) 1–39.
[5] C. Depcik, D. Assanis, One-dimensional automotive catalyst modeling, Prog. Energy Combust. Sci. 31 (2005) 308–369.
[6] S. Oh, J. Cavendish, Transients of monolithic catalytic converters: response to step changes in feedstream temperature as related to controlling automobile emissions, Ind. Eng. Chem. 21 (1982) 29–37.
[7] O. Lepreux, Model-based temperature control of a diesel oxidation catalyst, Ph.D. Thesis, École des Mines de Paris—MINES ParisTech (2009).
[8] A. Frobert, Y. Creff, O. Lepreux, L. Schmidt, S. Raux, Generating thermal conditions to regenerate a DPF: impact of the reductant on the performances of diesel oxidation catalysts, SAE Paper 2009-01-1085, April 2009.
[9] O. Lepreux, Y. Creff, N. Petit, Practical achievable performance in diesel oxidation catalyst temperature control, Oil Gas Sci. Technol.–Rev. IFP Energies nouvelles 66 (2011) 693–704.
[10] J.R. Cannon, The One-dimensional Heat Equation, Vol. 23 of Encyclopedia of Mathematics and its Applications, Addison-Wesley Publishing Company, 1984.
[11] O. Lepreux, Y. Creff, N. Petit, Model-based control design of a diesel oxidation catalyst, in: Proc. of ADCHEM 2009, International Symposium on Advanced Control of Chemical Processes, Istanbul, Turkey, 2009.
[12] M.N. Osizik, Basic Heat Transfer, McGraw-Hill, 1977.
[13] A.M. Il'in, The exponential boundary layer, in: M.V. Fedoryuk (Ed.), Partial Differential Equations V: Asymptotic Methods for Partial Differential Equations, Springer-Verlag, 1998 (Section V.1).